JCB Article

The GAP activity of Msb3p and Msb4p for the Rab GTPase Sec4p is required for efficient exocytosis and actin organization

Xiang-Dong Gao,[1] Stefan Albert,[2] Serguei E. Tcheperegine,[1] Christopher G. Burd,[1] Dieter Gallwitz,[2] and Erfei Bi[1]

[1]Department of Cell and Developmental Biology, University of Pennsylvania, Philadelphia, PA 19104
[2]Max Planck Institute for Biophysical Chemistry, Department of Molecular Genetics, D-37070 Göttingen, Germany

Polarized growth in *Saccharomyces cerevisiae* is thought to occur by the transport of post-Golgi vesicles along actin cables to the daughter cell, and the subsequent fusion of the vesicles with the plasma membrane. Previously, we have shown that Msb3p and Msb4p genetically interact with Cdc42p and display a GTPase-activating protein (GAP) activity toward a number of Rab GTPases in vitro. We show here that Msb3p and Msb4p regulate exocytosis by functioning as GAPs for Sec4p in vivo. Cells lacking the GAP activity of Msb3p and Msb4p displayed secretory defects, including the accumulation of vesicles of 80–100 nm in diameter. Interestingly, the GAP activity of Msb3p and Msb4p was also required for efficient polarization of the actin patches and for the suppression of the actin-organization defects in *cdc42* mutants. Using a strain defective in polarized secretion and actin-patch organization, we showed that a change in actin-patch organization could be a consequence of the fusion of mistargeted vesicles with the plasma membrane.

Introduction

Polarization of cell growth is critical for generating distinct cellular domains and is ultimately responsible for the diversity of cell types, tissues, and organs. Thus, cell polarity is essential for development and differentiation in many organisms (Drubin and Nelson, 1996). In the budding yeast *Saccharomyces cerevisiae*, polarized cell growth is thought to occur in a hierarchal manner. At the beginning of the cell cycle, the small Rho GTPase Cdc42p and its regulators such as the guanine nucleotide–exchange factor (GEF) Cdc24p are clustered at a specific region of the cell cortex, marking the site for polarity establishment (Johnson, 1999). Cdc42p effectors, including the p21-activated kinases, Ste20p and Cla4p; the formin, Bni1p; and the structurally related proteins, Gic1p and Gic2p; are then recruited to the cortical site to polymerize and/or organize the actin cytoskeleton, including actin cables and actin patches, at the presumptive bud site (Pruyne and Bretscher, 2000b). Actin patches are thought to mediate endocytosis (Munn, 2000), whereas actin cables are thought to function as tracks along which post-Golgi vesicles are transported from the mother cell to the daughter cell (Pruyne and Bretscher, 2000a).

Secretion in eukaryotes occurs in multiple, sequential steps, each of which is controlled by a distinct Rab GTPase. In *S. cerevisiae*, the Rab GTPase Sec4p plays a central role in polarized secretion from Golgi to the plasma membrane and is thought to act by tethering secretory vesicles to the plasma membrane via its effector, the exocyst, a multisubunit protein complex (Guo et al., 1999). Like other Ras-family members, Sec4p cycles between an inactive GDP- and active GTP-bound state. This cycling is regulated by its GEF, Sec2p (Walch-Solimena et al., 1997), and presumably by its GAP(s), whose identity has not been determined.

Msb3p and Msb4p are a pair of structurally related proteins that localize to the sites of polarized growth (Bi et al., 2000). Overexpression of Msb3p or Msb4p suppresses *cdc24*-Ts and *cdc42*-Ts mutants, although the mechanism underlying this suppression is not clear. Both Msb3p and Msb4p have a Rab GAP domain and indeed display a GAP activity toward a number of Rab GTPases in vitro (Albert and Gallwitz, 1999, 2000). However, the in vivo Rab targets of Msb3p and Msb4p are not known. In this report, we present multiple lines of evidence to indicate that Msb3p and Msb4p regulate exocytosis by functioning as GAPs for Sec4p in vivo. In contrast to the general view that polarized actin cytoskeleton guides secretion to a specific cellular domain, we also

Address correspondence to Erfei Bi, Department of Cell and Developmental Biology, University of Pennsylvania School of Medicine, Room 1012, BRB II/III, 421 Curie Blvd., Philadelphia, PA 19104-6058. Tel.: (215) 573-6676. Fax: (215) 898-9871. email: ebi@mail.med.upenn.edu

Key words: actin; exocytosis; Msb3p; Msb4p; Rab GAP

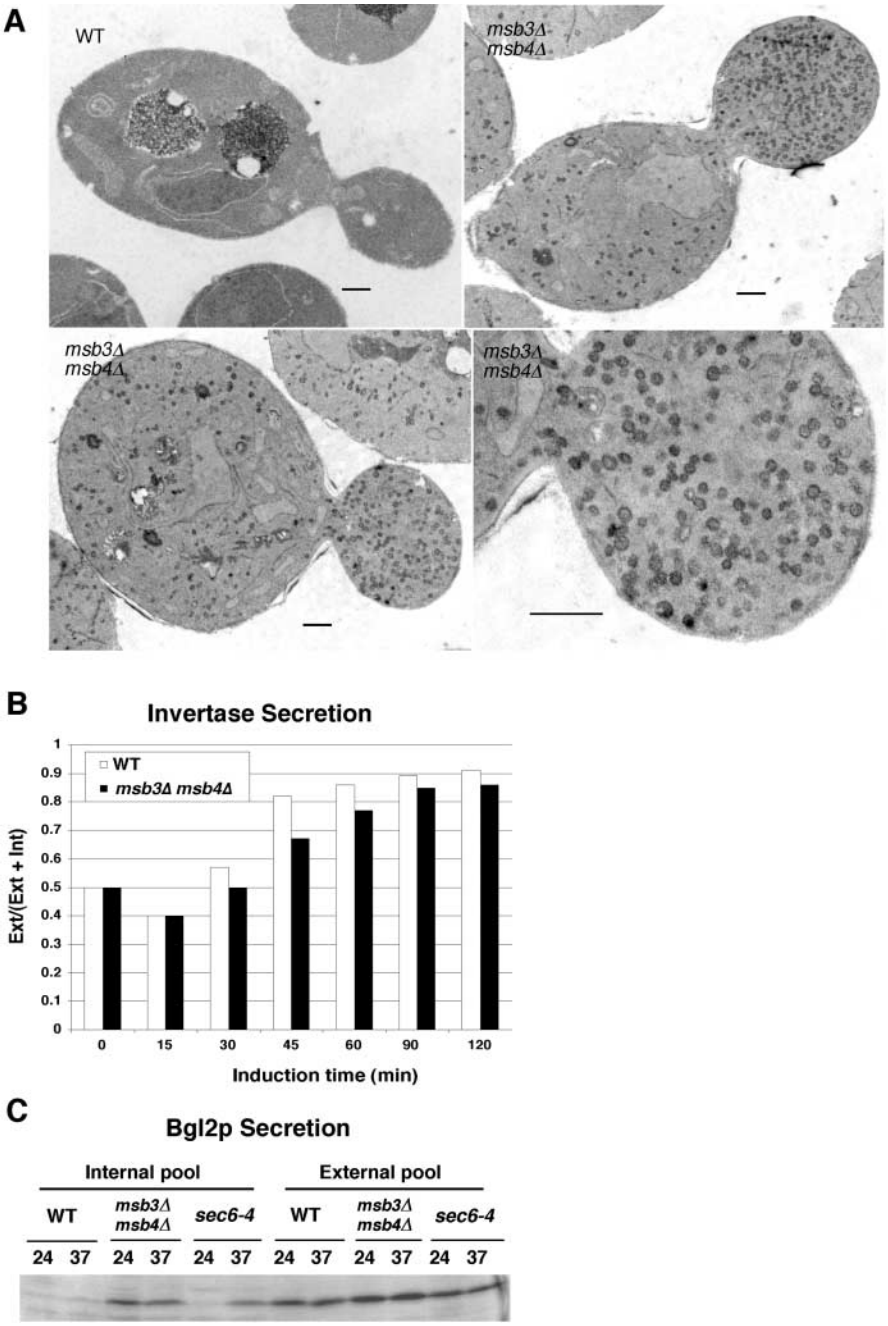

Figure 1. **Deletion of *MSB3* and *MSB4* causes a secretory defect.** (A) Wild-type (YEF473) and *msb3Δ msb4Δ* (YEF1631) cells were grown in YPD media at 24°C and processed for electron microscopy. Bars, 0.5 μm. (B) Invertase secretion. Wild-type (YEF473A) and *msb3Δ msb4Δ* (YEF1289) cells were induced for secretion of invertase at 24°C. The percentage of external (Ext, secreted) pool versus total invertase (Ext + Int) was measured at indicated times after induction. (C) Bgl2p secretion. Wild-type (YEF473A), *msb3Δ msb4Δ* (YEF1289) and *sec6–4* (BY37) cells were grown at 24°C, or shifted to 37°C for 1 h. The amounts of internal and external pools of Bgl2p were analyzed by Western blotting with anti-Bgl2p antibody. Samples of external pool were loaded only half the amount as those of internal pool.

present evidence to indicate that a primary defect in polarized secretion can cause defects in polarized actin organization. Thus, polarized actin organization and polarized secretion appear to reenforce each other.

Results

Deletion of *MSB3* and *MSB4* causes a secretory defect

Because Msb3p and Msb4p display a GAP activity toward a number of Rab GTPases in vitro, a substrate promiscuity that is common among most known Rab GAPs, we decided to define the in vivo Rab target(s) of Msb3p and Msb4p by the following approaches. First, we examined possible protein-trafficking defects in cells lacking both Msb3p and Msb4p. We found that *msb3Δ msb4Δ* cells accumulated a large number of vesicles at 24°C, whereas wild-type and single-mutant cells had none or very few vesicles (Fig. 1 A and Fig. 4 A). The vesicles were 90.00 ± 11.77 nm (n = 204) in diameter, falling within the range of 80–100 nm post-Golgi secretory vesicles (Novick and Schekman, 1979). In most cells, the vesicles appeared to be distributed randomly in the mother and the daughter (Fig. 1 A, bottom left). In a few cells, vesicles were concentrated in the daughter (Fig. 1 A, top right). These data suggest that Msb3p and Msb4p must share a function in secretion.

The second approach used to assess a possible secretory defect in *msb3Δ msb4Δ* cells was to monitor the secretion of invertase, a sucrose-metabolizing enzyme, and of Bgl2p, an endo-β-1,3-glucanase required for cell wall organization and biogenesis (Mrsa et al., 1993). When invertase secretion was

Table I. **Invertase secretion in wild-type and *msb3Δ msb4Δ* cells**

Induction time (min)	0	15	30	45	60	90	120
YEF473A (WT)							
Ext	0.02	0.02	0.04	0.09	0.12	0.16	0.20
Int	0.02	0.03	0.03	0.02	0.02	0.02	0.02
Ext/(Ext+Int)	0.50	0.40	0.57	0.82	0.86	0.89	0.91
YEF1289 (*msb3Δ msb4Δ*)							
Ext	0.02	0.02	0.03	0.12	0.20	0.35	0.49
Int	0.02	0.03	0.03	0.06	0.06	0.06	0.08
Ext/(Ext+Int)	0.50	0.40	0.50	0.67	0.77	0.85	0.86

Invertase activity (in units) was measured at different time points after induction at 24°C. Ext and Int stand for external (secreted) and internal pools of invertase, respectively.

followed over time at 24°C, the ratio of secreted invertase versus total invertase (external plus internal) was mildly, but consistently lower in *msb3Δ msb4Δ* cells than in wild-type cells, with the difference peaking around 45 min after induction (Fig. 1 B). However, the majority of invertase was secreted efficiently to the periplasmic region during the course of induction (Table I). In contrast, Bgl2p was accumulated in large quantity inside the *msb3Δ msb4Δ* cells at both 24°C and at 37°C (Fig. 1 C). As expected, Bgl2p accumulation in the late secretory mutant, *sec6–4*, was temperature dependent (Fig. 1 C). These data suggest that most vesicles accumulated in *msb3Δ msb4Δ* cells carry Bgl2p and a small fraction of vesicles carry invertase.

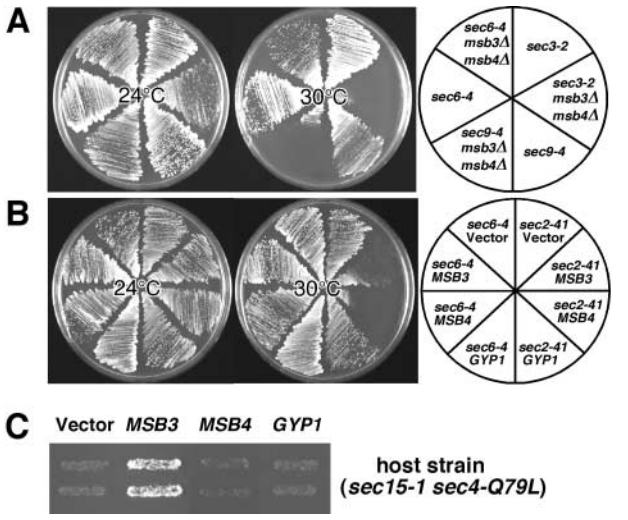

Figure 2. ***MSB3* and *MSB4* genetically interact with exocytosis genes and down-regulate *SEC4* function.** (A) Synthetic inhibitory effects on cell growth between *msb3Δ msb4Δ* and late *sec* mutants. Strains carrying *sec3–2* (JGY32B), *sec3–2 msb3Δ msb4Δ* (JGY37B), *sec9–4* (JGY31B), *sec9–4 msb3Δ msb4Δ* (JGY40A), *sec6–4* (JGY30A), and *sec6–4 msb3Δ msb4Δ* (JGY39A) were streaked onto YPD plates and incubated at 24°C for 3 d, or at 30°C for 2 d. (B) Multicopy *MSB3* or *MSB4* inhibits the growth of *sec2–41* cells. The *sec2–41* strain (JGY28B) and the control *sec6–4* strain (JGY30A) carrying plasmids YEplac181 (Vector), YEp181-MSB3, YEp181-MSB4, and YEp181-GYP1 were streaked onto SC-Leu plates and incubated at 24°C for 3 d, or at 30°C for 2 d. (C) Multicopy *MSB3* suppresses the lethality of the *sec15–1 s4-Q79L* double mutant. YEplac181 alone, or carrying 3HA-tagged *MSB3* or *MSB4*, or *GYP1*, was transformed into strain JGY86A (*sec15–1 s4-Q79L*, pRS316-SEC4). Transformants were replica-plated onto a SC-Leu+5FOA plate and incubated at 24°C for 3 d.

Genetic evidence for the involvement of Msb3p and Msb4p in exocytosis and for Msb3p and Msb4p functioning as GAPs for Sec4p in vivo

If Msb3p and Msb4p play a role in exocytosis, deletion or overexpression of *MSB3* and *MSB4* may display genetic interactions with some of the late secretory mutants. Indeed, deletion of *MSB3* and *MSB4* produced synthetic inhibitory effects on cell growth with *sec3–2* and *sec9–4* mutants at 30°C, but not with *sec1–1*, *sec2–41*, *sec4–8*, and *sec6–4* mutants (Fig. 2 A). In addition, overexpression of Msb3p or Msb4p inhibited the growth of *sec2–41* cells at 30°C, but not of any other late *sec* mutants, including *sec1–1, sec3–2, sec4–8, sec5–24, sec6–4, sec8–9, sec9–4, sec10–2,* and *sec15–1* (Fig. 2 B). In contrast, overexpression of Gyp1p, a GAP for Ypt1p that is involved in ER to Golgi transport but also exhibits a GAP activity toward Sec4p in vitro (Du et al., 1998; Du and Novick, 2001; De Antoni et al., 2002), did not inhibit the growth of *sec2–41* cells at 30°C (Fig. 2 B). These results suggest that Msb3p and Msb4p are involved in exocytosis and can antagonize the function of Sec2p, the known GEF for Sec4p.

Because Msb3p and Msb4p display a GAP activity toward Sec4p in vitro and appear to colocalize with Sec4p at the sites of polarized growth during the cell cycle, it seemed likely that Msb3p and Msb4p might participate in the regulation of exocytosis by functioning as GAPs for Sec4p in vivo. To test this hypothesis, we took advantage of the observation that a *sec4-Q79L sec15–1* double mutant is inviable at 25°C (Walworth et al., 1992). The Q79L mutation shifts Sec4p toward its GTP-bound form by decreasing the intrinsic GTPase activity, but this Sec4p mutant is still responsive to GAP action (Walworth et al., 1992; Du et al., 1998). Sec15p, an effector of Sec4p, is thought to mediate the role of Sec4p in the assembly of the exocyst (Guo et al., 1999). We reasoned that if Msb3p and Msb4p are physiological GAPs for Sec4p, their overexpression might suppress the synthetic lethality between *sec4-Q79L* and *sec15–1* by decreasing the level of GTP-bound Sec4p.

To examine this possibility, we constructed a *sec4-Q79L sec15–1* double mutant harboring an *URA3*-marked plasmid carrying wild-type *SEC4*. A *LEU2*-marked multicopy plasmid carrying either *MSB3* or *MSB4* was transformed into the tester strain and assayed for its ability to replace the *SEC4*-containing plasmid by examining cell growth on plates containing 5FOA, a chemical that selects for cells that have lost the *URA3*-containing plasmid (Fig. 2 C). Multicopy *MSB3*, but not *GYP1* or *MSB4*, was able to suppress the *sec4-Q79L sec15–1* mutant, supporting the hypothesis that Msb3p functions as a GAP for Sec4p in vivo.

Msb3p and Msb4p function as GAPs for Sec4p by an arginine finger–like mechanism

GAPs for Ras, Rho, and Rab GTPases all contain an invariant arginine residue (the "finger arginine") in the catalytic domain that is critical for their GAP activities (Ahmadian et al., 1997; Albert et al., 1999). Because Msb3p and Msb4p

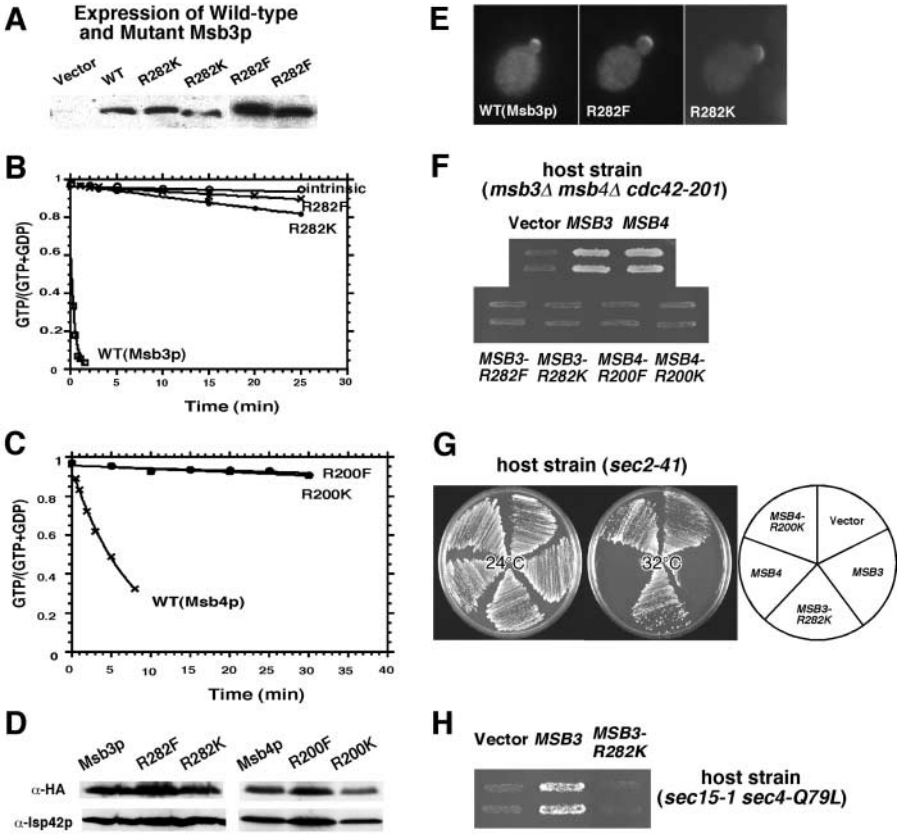

Figure 3. **Msb3p and Msb4p function as GAPs for Sec4p by an arginine finger-like mechanism.** (A) Crude extracts from yeast cells overexpressing His_6-tagged Msb3p wild-type (WT) or arginine mutants were analyzed by Western blotting with anti-His_6 antibody. (B and C) Time course of hydrolysis of Sec4p-bound GTP stimulated by the wild-type or the arginine mutants of Msb3p (B) or by the wild-type or the arginine mutants of Msb4p (C). (D) The arginine mutants of Msb3p and Msb4p express normally. Yeast strain JGY18 (*msb3Δ msb4Δ cdc42–201*, pRS316-CDC42) carrying plasmid YEp181–3HA-MSB3, YEp181–3HA-MSB3-R282F, YEp181–3HA-MSB3-R282K, YEp181–3HA-MSB4, YEp181–3HA-MSB4-R200F, or YEp181–3HA-MSB4-R200K was analyzed for the expression of wild-type and the arginine mutants of Msb3p and Msb4p. The mitochondrial outer membrane protein Isp42p was used as a loading control. (E) The arginine mutants of Msb3p localize normally. YEp181–3HA-MSB3, YEp181–3HA-MSB3-R282F, or YEp181–3HA-MSB3-R282K was transformed into YEF1619 (*msb3Δ/msb3Δ*). Transformants were grown at 24°C and processed for immunofluorescence with anti-HA antibody. (F) The GAP activity of Msb3p and Msb4p is required for their in vivo function. YEplac181 alone, or carrying 3HA-tagged *MSB3*, *MSB4*, or their respective arginine mutants, was transformed into strain JGY18 (*msb3Δ msb4Δ cdc42–201*, pRS316-CDC42). Transformants were replica plated onto a SC-Leu+5FOA plate and incubated at 24°C for 4 d. (G) The GAP activity of Msb3p and Msb4p is required for their inhibitory effects on a *sec2–41* mutant. YEplac181 alone, or carrying *3HA-MSB3*, *3HA-msb3-R282K*, *3HA-MSB4*, *3HA-msb4-R200K* was transformed into JGY28B (*sec2–41*). Transformants were streaked onto SC-Leu plates and incubated for 3 d at 24°C, or for 2 d at 32°C. (H) The GAP activity of Msb3p is required for the suppression of the *sec15–1 s4-Q79L* mutant. YEplac181 alone, or carrying *3HA-MSB3* or *3HA-msb3-R282K*, was transformed into strain JGY86A (*sec15–1 s4-Q79L*, pRS316-SEC4). Transformants were replica plated onto a SC-Leu+5FOA plate and incubated at 24°C for 3 d.

contain an arginine residue (R282 in Msb3p and R200 in Msb4p) at the corresponding position, we decided to examine whether Msb3p and Msb4p function on Sec4p by a similar mechanism. In addition, we hoped that Msb3p and Msb4p mutants deficient in the GAP activity toward Sec4p might offer an opportunity to distinguish the role of Msb3p and Msb4p in secretion from their role in actin organization. For these reasons, we substituted the arginine residue in Msb3p and Msb4p for either phenylalanine or lysine and determined the properties of the mutant proteins.

To facilitate protein purification, Msb3p, Msb4p, and their derivatives were all tagged with six histidines at their COOH termini. The tagged Msb3p and the arginine mutants were expressed from a galactose-inducible promoter in yeast cells. Crude extracts containing induced Msb3p or its mutant forms were subjected to a filter assay with GTP-loaded Sec4p as a substrate. Only extracts from cells overexpressing wild-type Msb3p exhibited measurable GAP activity (unpublished data), even though the mutant proteins, Msb3p-R282F and Msb3p-R282K, and the wild-type protein were expressed at similar levels (Fig. 3 A). For a quantitative assay, Msb3p and its mutants were purified from induced cells by affinity chromatography and assayed for their GAP activities toward GTP-loaded Sec4p by an HPLC-based method. As shown in Fig. 3 B, in comparison to wild-type Msb3p, both arginine mutants showed a significantly reduced Sec4p-GAP activity.

Msb4p and its mutants, Msb4p-R200F and Msb4p-R200K, were purified from *E. coli* cells and tested with GTP-loaded Sec4p as a substrate (Fig. 3 C). Again, the arginine mutation led to a significant loss of GAP activity. These data suggest that Msb3p and Msb4p function as GAPs for Sec4p by an arginine finger-like mechanism.

The GAP activity of Msb3p and Msb4p is essential for their in vivo function

Despite the drastic reduction in their GAP activity toward Sec4p, the arginine mutants of Msb3p and Msb4p were expressed at normal levels (Fig. 3 D) and localized to the sites of polarized growth like the wild-type proteins (Fig. 3 E, and unpublished data). These data suggest that a significant loss of the GAP activity of Msb3p and Msb4p does not compromise the molecular interactions required for their targeting to the growth sites.

To determine whether the GAP activity of Msb3p and Msb4p is required for their in vivo function, we developed two assays. The first assay is based on our previous observation that *msb3Δ msb4Δ gic1Δ gic2Δ* quadruple mutant is in-

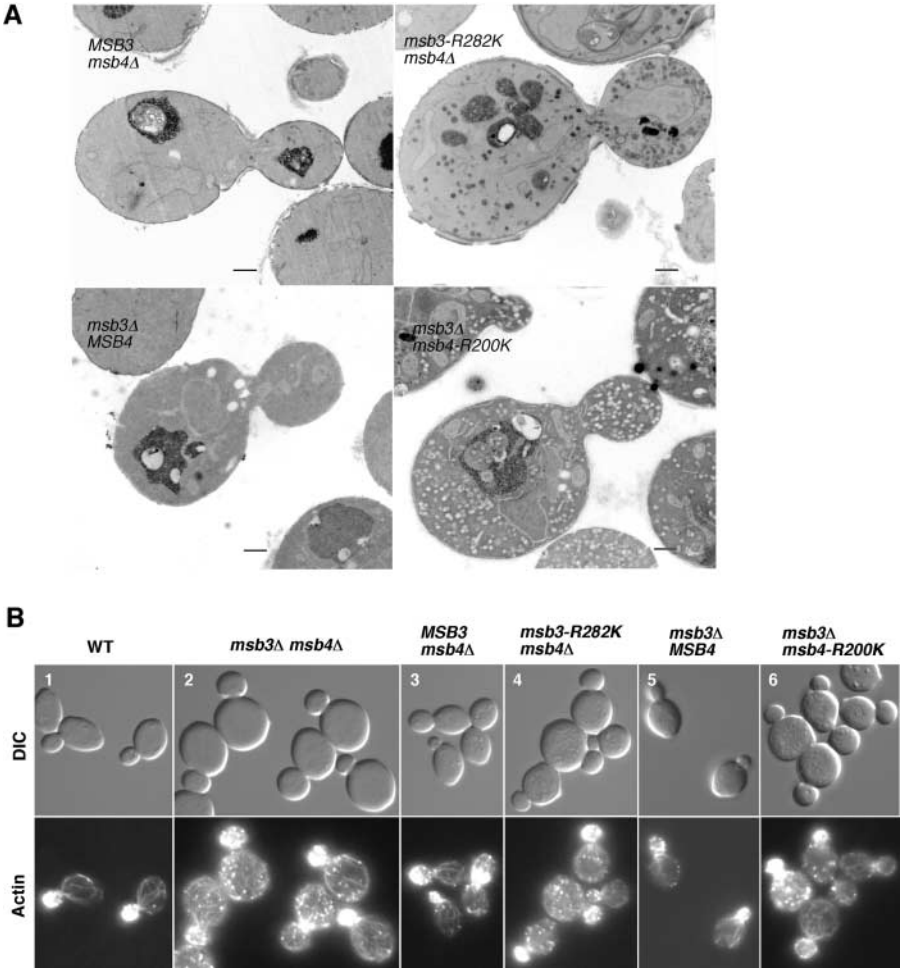

Figure 4. **Loss of the GAP activity of Msb3p and Msb4p causes vesicle accumulation and a defect in actin organization.** (A) *MSB3 msb4Δ* (JGY184A), *msb3-R282K msb4Δ* (JGY190A), *msb3Δ MSB4* (JGY51), and *msb3Δ msb4-R200K* (JGY127A) cells were grown in YPD media at 24°C and processed for electron microscopy. Please note that the appearance of vesicles varies from batch to batch due to possible variations in sample preparations. Bars, 0.5 μm. (B) Wild-type (YEF473), *msb3Δ msb4Δ* (YEF1631), *MSB3 msb4Δ* (JGY184), *msb3-R282K msb4Δ* (JGY190), *msb3Δ MSB4* (JGY71), and *msb3Δ msb4-R200K* (JGY130) diploid cells were grown at 24°C and stained for F-actin.

viable with a loss-of-polarity phenotype (Bi et al., 2000). The second assay is based on our new observation that *msb3Δ msb4Δ* is synthetically lethal with *cdc42–201*, a newly isolated temperature-sensitive *cdc42* allele (Zhang et al., 2001). These two tester strains were kept alive by introducing an *URA3*-marked plasmid that carries either wild-type *GIC1* for the first assay or *CDC42* for the second assay. HA-tagged Msb3p, Msb4p, and their arginine mutants expressed from a *LEU2*-marked, high-copy plasmid in the tester strains were assayed for their ability to replace the *URA3*-marked plasmids on SC-Leu+5FOA plates. Plasmids carrying the arginine mutants of *MSB3* or *MSB4* failed to replace the *URA3*-marked plasmids in both assays, in direct contrast to the plasmids carrying wild-type *MSB3* or *MSB4* (Fig. 3 F and unpublished data). These data indicate that the GAP activity of Msb3p and Msb4p is essential for their in vivo function(s).

Overexpression of Msb3p-R282K and Msb4p-R200K mutants also failed to inhibit the growth of *sec2–41* cells at

Table II. **The GAP activity of Msb3p is required for the suppression of the actin-organization defects in *cdc42*-Ts mutants**

Plasmids	YEF115 (*cdc42-1*) host strain				YEF2258 (*cdc42-201*) host strain			
	(24°C) 0 min		38.5°C 5.3 h		(24°C) 0 min		35.5°C 6 h	
	Budded cells	Actin polarized	Budded cells	Actin polarized	Budded cells	Actin polarized	Budded cells	Actin polarized
	%	%	%	%	%	%	%	%
YEplac181	3	8	6	20	5	3	8	6
YEp181-3HA-MSB3	4	9	42	75	6	4	48	38
YEp181-3HA-MSB3-R282K	5	10	13	39	7	3	7	6
YEp181-3HA-MSB1	4	6	29	60	7	3	20	19

The enriched, unbudded population of cells harboring indicated plasmids were grown in fresh media at indicated temperatures for the indicated lengths of time before assaying for the suppression of the budding and the actin-organization defects (see Materials and methods for detail). More than 600 cells were scored to determine the percentage of budded cells by DIC microscopy, and at least 200 cells were scored for actin organization through F-actin staining. Shown here is one set of representative results from three independent experiments performed in each *cdc42*-Ts host strain. Representative cells are shown in Fig. 5 B.

32°C (Fig. 3 G), suggesting that the GAP activity of Msb3p and Msb4p is required for antagonizing the function of Sec2p. The arginine mutant of Msb3p also failed to suppress the synthetic lethality between *sec4-Q79L* and *sec15–1* (Fig. 3 H), further supporting the notion that it is the GAP activity of Msb3p toward Sec4p, not merely the presence of Msb3p, that is responsible for the suppression.

The GAP activity of Msb3p and Msb4p is required for efficient exocytosis and polarized actin organization

To determine whether vesicle accumulation in *msb3Δ msb4Δ* cells was due to the absence of the proteins or the loss of their GAP activity, we examined two pairs of haploid strains, JGY184A (*MSB3 msb4Δ*) and JGY190A (*msb3-R282K msb4Δ*), and JGY51 (*msb3Δ MSB4*) and JGY127A (*msb3Δ msb4-R200K*). In most *MSB3 msb4Δ* or *msb3Δ MSB4* cells, either no or just a few vesicles (usually <10 vesicles per cell section) were detected (Fig. 4 A, left). In contrast, most *msb3-R282K msb4Δ* or *msb3Δ msb4-R200K* cells accumulated a large number of vesicles similar to those observed in *msb3Δ msb4Δ* cells (Fig. 4 A, right). These data indicate that the loss of the GAP activity of Msb3p and Msb4p is responsible for vesicle accumulation.

Cells of *msb3Δ msb4Δ* strain are rounder in shape, heterogeneous in size, and have a partially disrupted actin cytoskeleton (Bi et al., 2000). Actin patches in these cells tended to delocalize into the mother side at early stages of the cell cycle when the patches should be predominantly concentrated in the buds (Fig. 4 B, compare columns 1 and 2). Actin cables were clearly present and largely well organized in *msb3Δ msb4Δ* cells. However, some cables appeared to be shorter, and sometimes misoriented in the mutant strain (Fig. 4 B, compare columns 1 and 2).

To determine whether the GAP activity of Msb3p and Msb4p is required for actin-patch organization, *MSB3*, *msb3-R282K*, *MSB4*, or *msb4-R200K* was integrated into the *msb3Δ msb4Δ* mutant at the *msb3Δ* or *msb4Δ* locus, respectively. The integrants with *MSB3* or *MSB4* showed normal cell morphology and actin-patch organization (Fig. 4 B, columns 3 and 5). Interestingly, the integrants with *msb3-R282K* or *msb4-R200K* displayed similar defects in cell morphology and actin-patch organization as the *msb3Δ msb4Δ* mutant did (Fig. 4 B, columns 4 and 6), suggesting that the GAP activity of Msb3p and Msb4p is required for actin-patch organization.

Multicopy *MSB3* is known to suppress the growth defect of *cdc42–1* cells at the nonpermissive temperature (Bi et al., 2000) (Fig. 5 A, top). We found that multicopy *MSB3* also suppressed the growth defect of another *cdc42*-Ts allele, *cdc42–201* (Fig. 5 A, bottom). In addition, the budding and the actin-organization defects in both *cdc42*-Ts mutants were largely suppressed by multicopy *MSB3* (Fig. 5 B) (Table II). Interestingly, multicopy *msb3-R282K* failed to suppress both the budding and the actin-organization defects of the two *cdc42*-Ts mutants (Fig. 5, A and B) (Table II), which were not defective in secretion per se as indicated by EM studies (Fig. 5 C). These results suggest that the GAP activity of Msb3p is required for the suppression of the actin-organization defects in *cdc42* mutants. Together with the results described in the previous section, these data raise an intriguing

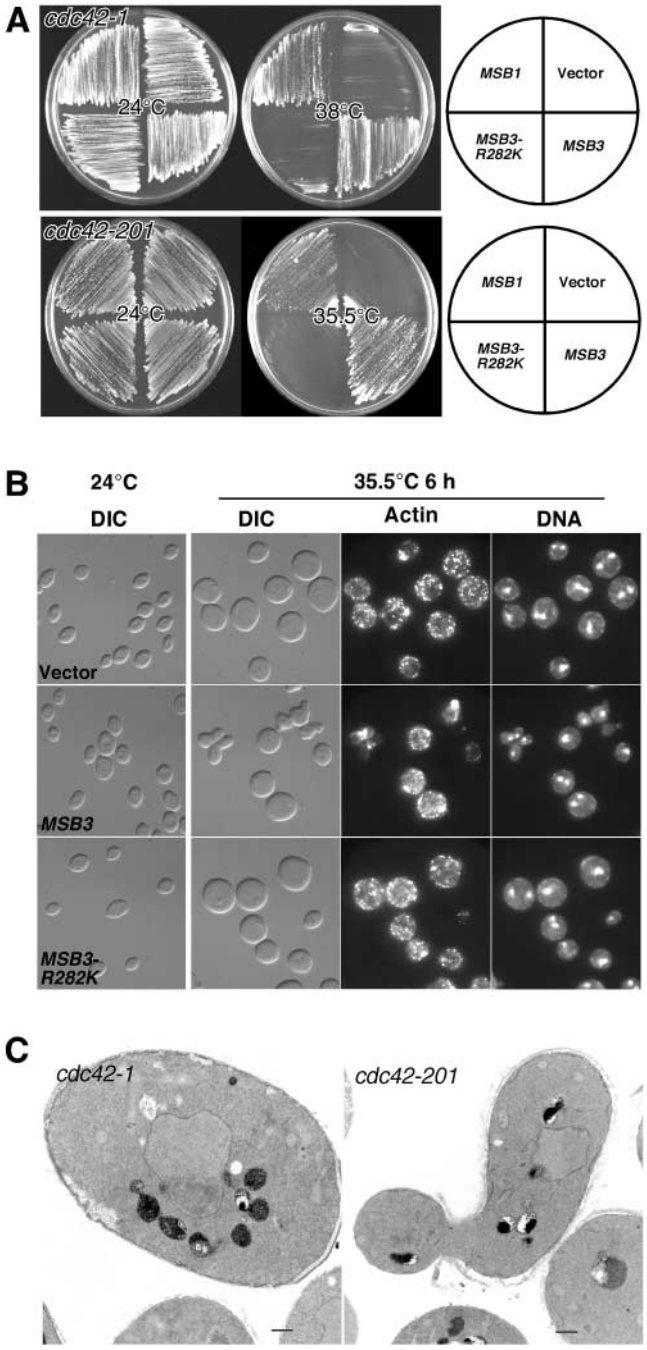

Figure 5. **The GAP activity of Msb3p is required for the suppression of the budding and the actin-organization defects in *cdc42*-Ts mutants.** (A) YEplac181 alone, or carrying *3HA-MSB3* or *3HA-msb3-R282K* or *3HA-MSB1* (*MSB1*, a known multicopy suppressor of *cdc42–1* [Bender and Pringle, 1989], serves as a control here), was individually transformed into strains YEF115 (*cdc42–1*) and YEF2258 (*cdc42–201*), respectively. Transformants were streaked onto SC-Leu plates and incubated for 3 d at 24°C, or for 2 d at 38°C (for *cdc42–1* host) and at 35.5°C (for *cdc42–201* host). (B) The unbudded population of *cdc42–201* cells carrying YEplac181, YEp181–3HA-MSB3, or YEp181–3HA-MSB3-R282K were enriched and released into SC-Leu medium at 35.5°C. Cells were fixed and stained for F-actin and DNA. Representative cells before shifting (24°C) and after shifting (35.5°C 6 h) were shown (see also Table II). (C) YEF115 (*cdc42–1*) and YEF2258 (*cdc42–201*) cells were grown in YPD media at 24°C, and then shifted to 37.5°C and 36°C for 1 h, respectively. Cells were processed for electron microscopy. Bars, 0.5 μm.

A The Percentage of Small-budded Cells With Polarized Actin Patches

Yeast strains	0 min	30 min	60 min
tpm2Δ	100%	39%	88%
tpm1-2 tpm2Δ	100%	3%	0%
sec6-4 tpm1-2 tpm2Δ	100%	73%	51%
sec6-4	100%	75%	85%

C The Lifespan of Actin Patches (sec)

Yeast strains	20°C	36°C
tpm2Δ	16±4	9±3
tpm1-2 tpm2Δ	16±3	8±2
sec6-4 tpm1-2 tpm2Δ	16±3	21±7
sec6-4	17±3	21±8

B

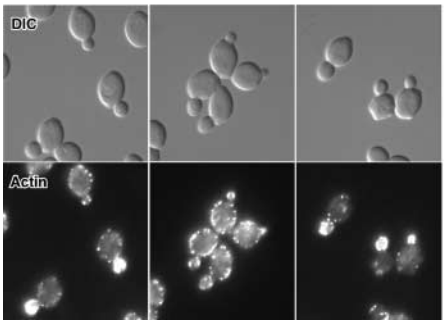

D

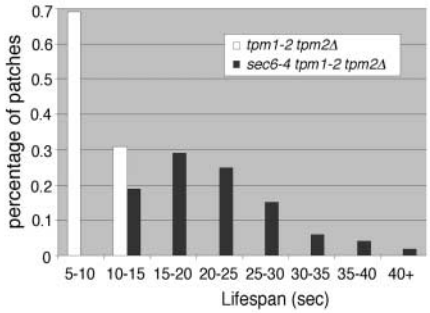

Figure 6. **Blocking of vesicle fusion with the plasma membrane prevents the reorganization of actin patches into the mother compartment in cells lacking actin cables.** (A and B) Strains *tpm2Δ* (ABY973), *tpm1–2 tpm2Δ* (ABY971), *sec6–4 tpm1–2 tpm2Δ* (ABY999), and *sec6–4* (JGY381) carrying *GFP-TUB1* were grown in YPD media at 24°C and then shifted to 36°C for 0, 30, and 60 min. Cells were fixed and stained for F-actin. (A) The percentage of small-budded cells that displayed a polarized distribution of actin patches after shifting to 36°C for different periods of time was shown. (B) Representative cells shifted to 36°C for 60 min were shown. (C) The same strains as in A, except carrying *ABP1-GFP* instead of *GFP-TUB1*, were grown at 20°C. The lifespan (in seconds) of actin patches in each strain was measured in time-lapse series at 20°C, and at 36°C after shifting to 36°C for 60 min. At least 100 actin patches from both the mother and the daughter compartments of budded cells were analyzed for each strain at each temperature. (D) The percentage distribution of actin-patch lifespan in strains *tpm1–2 tpm2Δ* (ABY971) and *sec6–4 tpm1–2 tpm2Δ* (ABY999) at 36°C.

possibility that polarized secretion may be normally involved in modulating polarized actin organization.

A defect in actin-patch organization can be a consequence of a primary defect in polarized secretion

The fact that the GAP activity of Msb3p is required to rescue both the secretory and the actin-patch-organization defects in *msb3Δ msb4Δ* cells raises the possibility that the actin-patch disorganization in *msb3Δ msb4Δ* cells might be a consequence of the fusion of mistargeted vesicles with the plasma membrane of the mother cells. To examine this possibility, we took advantage of mutants in *TPM1* and *TPM2*, which encode two isoforms of tropomyosin that are required specifically for the formation of actin cables but not actin patches (Pruyne et al., 1998). When tropomyosins are conditionally inactivated, all actin cables are lost within one minute. As a result, secretory vesicles are no longer transported to the daughter cell, but instead fuse with the plasma membrane of the mother cell. After inactivation of tropomyosins for 30–60 min, actin patches become randomly distributed in both the mother and the daughter cells (Fig. 6, A and B) (Pruyne et al., 1998).

To test our hypothesis, we examined the distribution of actin patches in *sec6–4 tpm1–2 tpm2Δ* cells. At the restrictive temperature, secretory vesicles in this mutant are no longer delivered to the bud due to the loss of actin cables. In addition, vesicles in this mutant fail to fuse with the plasma membrane due to the inactivation of Sec6p, a component of the exocyst that is essential for vesicle tethering. We observed that, upon shifting to 36°C for 60 min, 51% of the triple mutant cells still displayed a polarized organization of actin patches in comparison to 88% of the *tpm2Δ* cells, 85% of the *sec6–4* cells, and 0% of the *tpm1–2 tpm2Δ* cells (Fig. 6, A and B). These results suggest that the actin-patch disorganization in *tpm1–2 tpm2Δ* cells, and, by extrapolation, in *msb3Δ msb4Δ* cells, depends on the fusion of secretory vesicles in the mother cells with the plasma membrane.

One possible explanation for the polarized organization of actin patches in *sec6–4 tpm1–2 tpm2Δ* cells is that the lifespan of the "old patches" (existed before the temperature shift) in the buds of the small-budded cells is significantly increased. We measured the lifespan of actin patches in four different strains at two different temperatures, 20°C and 36°C, using Abp1p-GFP as a marker for the patches (Fig. 6, C and D). At 20°C, actin patches in all four strains displayed a similar lifespan, ~16 s. At 36°C, the lifespan of actin patches in both tropomyosin mutants (*tpm2Δ* and *tpm1–2 tpm2Δ*) were ~9 s. In contrast, the lifespan of actin patches in both mutants carrying *sec6–4* (*sec6 tpm1–2 tpm2Δ*, and *sec6–4*) were ~21 s. We also observed that the lifespan of actin patches in the mother and the daughter compartments of the same cell were virtually identical for all four strains at both temperatures. These data suggest that blocking exocytosis at 36°C increases the lifespan of actin patches, but this increase alone is not sufficient to explain the polarized actin-patch organization in the *sec6 tpm1–2 tpm2Δ* mutant.

Discussion

Msb3p and Msb4p are involved in exocytosis by functioning as GAPs for Sec4p in vivo

The challenge for studying Rab GAPs is twofold. First, most Rab GAPs in yeast are not essential for cell viability. Cells

lacking a single known Rab GAP in yeast, Gyp1p, Mdr1p/Gyp2p, Gyp5p, Gyp6p, Gyp7p, or Gyp8p, produce no obvious defects in protein trafficking (Strom et al., 1993; Vollmer and Gallwitz, 1995; Du et al., 1998; Albert and Gallwitz, 1999; Vollmer et al., 1999; Du and Novick, 2001; De Antoni et al., 2002). Second, all known Rab GAPs show substrate promiscuity in in vitro assays, and with the exception of Ypt1p-GAPs (Du and Novick, 2001; De Antoni et al., 2002), no evidence for their in vivo function has been obtained.

We took multiple approaches to assess whether Msb3p and Msb4p are Sec4p-specific GAPs in vivo. First, deletion of *MSB3* and *MSB4* together, more specifically, inactivation of the GAP activity of Msb3p and Msb4p caused a defect in exocytosis. Second, *msb3Δ msb4Δ* cells displayed synthetic interactions with late secretory mutants. Third, multicopy *MSB3* suppressed the synthetic lethality of a *sec4-Q79L sec15–1* mutant, presumably, by reducing the level of GTP-bound Sec4p. Fourth, multicopy *MSB3* or *MSB4* inhibited the growth of *sec2–41* cells, but not of any other late *sec* mutants. Finally, among the 11 Rab GTPases in *S. cerevisiae*, only Sec4p shares a localization profile and mutant phenotype (post-Golgi vesicle accumulation and exocytosis defect) with Msb3p and Msb4p. We further demonstrate here that Msb3p and Msb4p most likely act on Sec4p by an arginine finger–like mechanism. Together, these results provide compelling arguments for the involvement of Msb3p and Msb4p in exocytosis by functioning as GAPs for Sec4p in vivo.

Deletion of *MSB3* and *MSB4*, presumably leading to a higher level of Sec4p-GTP in the cell, caused significant accumulation of 100-nm vesicles and of the endoglucanase Bgl2p in the cell, but produced little effect on invertase secretion. A similar effect on invertase secretion is also observed in a strain carrying *sec4-Q79L*, in which Sec4p is predominantly in the GTP-bound form (Walworth et al., 1992). These data suggest that a defect in GTP hydrolysis by Sec4p affects secretion of different cargoes differentially, which is consistent with a previous report that there are at least two distinct populations of post-Golgi vesicles accumulated in late *sec* mutants: a minor population carries invertase, whereas the major population carries Bgl2p (Harsay and Bretscher, 1995). Similar differential effect on secretion is also observed in a *cdc42*-Ts mutant (Adamo et al., 2001). Because Msb3p, Msb4p, and Cdc42p are all involved in polarized growth and because Msb3p and Msb4p interact with Cdc42p genetically (Bi et al., 2000) and biochemically (unpublished data), it is possible that one role of Msb3p, Msb4p, and Cdc42p in polarized growth is to regulate secretion of Bgl2p, a cell wall–remodeling enzyme that is needed during cell-surface expansion.

The GAP activity of Msb3p and Msb4p and its implication in spatial regulation of exocytosis

Our EM studies indicate that in most *msb3 msb4* mutant cells, vesicles are distributed randomly within the cell, and in a few cells, vesicles are preferentially localized to the daughter cell. This pattern of vesicle accumulation would be consistent with a defect in vesicle transport and/or tethering. Vesicle transport from Golgi membrane to bud tip requires the function of vesicle-associated Sec4p-GTP, whose formation is catalyzed by the vesicle-associated GEF Sec2p, presumably using the cytosolic pool of Sec4p-GDP as the substrate. Vesicle tethering requires the function of Sec4p-GTP and its effector, the exocyst (Guo et al., 1999). In the absence of Msb3p and Msb4p, Sec4p would be primarily in the GTP-bound form and less Sec4p-GDP would be recycled back to the cytosol. This raises the question as to how an alteration in the ratio of GTP-bound versus GDP-bound Sec4p results in vesicle accumulation. We imagine two major scenarios. First, the decreased recycling of Sec4p-GDP to the cytosol in *msb3 msb4* mutant cells could be responsible for the vesicle accumulation. In this case, less Sec4p-GDP from the cytosol is recruited to the Golgi site to be converted to Sec4p-GTP on Golgi membranes and/or vesicles. Consequently, the efficiency of vesicle transport is compromised. The second scenario is that the increased amount of Sec4p-GTP in *msb3 msb4* mutant cells could be responsible for the vesicle accumulation. In this case, the increased level of Sec4p-GTP might hold the exocyst in place for longer periods of time so that reduced recycling of exocyst components would cause a defect in additional rounds of vesicle tethering. It is also possible that the disassembly of the vesicle-tethering complex is a prerequisite for the formation of the trans-SNARE complexes between Golgi membrane–derived vesicles and the plasma membrane, which leads to vesicle fusion. Because the assembly of the exocyst depends on Sec4p-GTP (Guo et al., 1999), its disassembly may depend on the hydrolysis of Sec4p-bound GTP. Thus, a deficiency in GTP hydrolysis may cause a secretory defect by indirectly preventing efficient formation of the SNARE complexes.

To distinguish between the two scenarios, we reasoned that, if the Sec4p-GDP recycling is the key, multicopy wild-type *SEC4* should suppress the morphological defect of the *msb3Δ msb4Δ sec4-Q79L* mutant, because more Sec4p-GDP would be generated in the cell due to the intrinsic GTPase activity of the wild-type Sec4p. In contrast, if the absolute amount of Sec4p-GTP is critical, multicopy *SEC4* should exacerbate the morphological defect of the *msb3Δ msb4Δ sec4-Q79L* mutant, because more Sec4p-GTP would be produced in the cell due to the increased concentration of Sec4p protein. We found that multicopy *SEC4* suppressed the morphological defect of the triple mutant reasonably well (unpublished data), thus favoring the first scenario. However, this result cannot rule out the second scenario with certainty.

The cellular locations of the GEF and the GAPs for Sec4p provide direct clues on how the activity of Sec4p, and hence the exocytosis, is spatially regulated (Fig. 7 A). Sec2p, the GEF for Sec4p, colocalizes with Sec4p on the secretory vesicles. This colocalization is thought to ensure Sec4p in its GTP-bound form, which is required for the transport of post-Golgi vesicles to the active growth sites (Walch-Solimena et al., 1997). In contrast, Msb3p and Msb4p, the GAPs for Sec4p, are mainly concentrated at the active growth sites in close association with the plasma membrane. This conclusion is based on cell-fractionation and localization studies on Msb3p and Msb4p (Bi et al., 2000) (unpublished data). Thus, Msb3p and Msb4p are well positioned to promote efficient recycling of Sec4p by facilitating the hydrolysis of Sec4p-bound GTP at the plasma membrane.

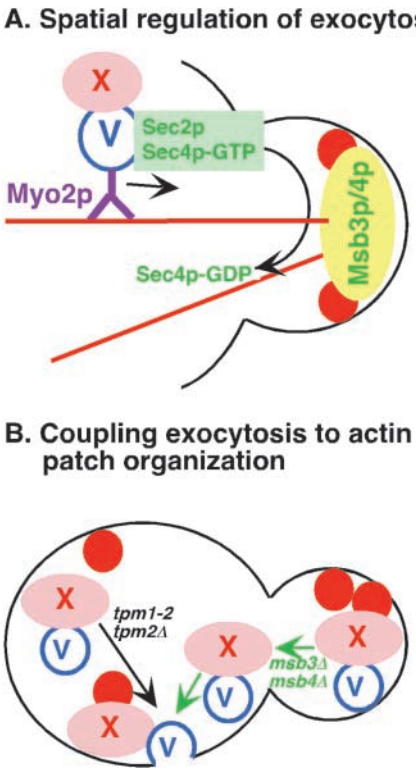

Figure 7. **Models on the spatial regulation of exocytosis and on the coupling of exocytosis to actin-patch organization.** (A) Role of Msb3p and Msb4p in spatial regulation of exocytosis. Secretory vesicles carrying Sec4p-GTP, Sec2p (GEF for Sec4p), and actin-patch clustering and/or assembly factor X are delivered to the bud tip by Myo2p (a type V myosin) along actin cables. Msb3p and Msb4p at the bud tip stimulate the hydrolysis of Sec4p-bound GTP, leading to the recycling of Sec4p for next round of exocytosis. The cargo molecule X, which could include the polarity proteins Cdc42p, Rho1p, and the actin-binding protein Aip3p/Bud6p, is delivered to the bud tip to reenforce the polarized organization of actin patches, which, in turn, may be involved in the recycling of the exocytic machinery such as the exocyst for next round of secretion. (B) Fusion of an exocytic vesicle with the plasma membrane leads to the formation and/or trapping of an actin patch at the fusion site. In *msb3Δ msb4Δ* cells, vesicles that are not transported out of the mother compartment can fuse with the plasma membrane (not depicted in the diagram). Vesicles that are not tethered at the bud tip (green arrows) can diffuse into the mother side and fuse with the plasma membrane, depositing their cargoes, including factor X, at the fusion sites for the generation and/or trapping of actin patches. In a tropomyosin mutant (black arrow), the vesicles are not transported to the bud and thus fuse with the plasma membrane of the mother compartment, leading to the reorganization of actin patches as described for *msb3Δ msb4Δ* cell.

A defect in polarized secretion can lead to a defect in polarized actin organization

Our studies led to two interesting findings. First, the GAP activity of Msb3p and Msb4p is required for efficient exocytosis and actin-patch organization. Second, the GAP activity of Msb3p is required for the suppression of the actin-organization defects in *cdc42–1* and *cdc42–201* cells. These observations raise an intriguing question: could a defect in polarized secretion cause a defect in actin organization? In *tpm1–2 tpm2Δ* cells where actin cables are absent at 36°C, secretory vesicles fuse with any part of the plasma membrane, causing depolarized growth. Meanwhile, actin patches are gradually reorganized from the small buds to the entire cell cortex (Pruyne et al., 1998). However, when the actin cables and the vesicle-tethering/fusion process are simultaneously inactivated in the *sec6–4 tpm1–2 tpm2Δ* cells, actin patches remain in the small buds. This result suggests that the reorganization of actin patches in *tpm1–2 tpm2Δ* cells depends on ongoing exocytosis and, likely, endocytosis, both of which are defective in *sec6–4* and all other late *sec* mutants (Riezman, 1985).

Actin-patch polarization in the small buds of the *sec6–4 tpm1–2 tpm2Δ* cells at 36°C can be explained by one of the three possibilities: patch motility is blocked; the lifespan of the patches is increased dramatically; and the putative patch-clustering factor and/or patch-assembly factor remains in the small bud in the absence of continuous exocytosis and endocytosis. Our data support the third possibility.

Patch motility is unlikely to be the answer. First, patches are highly labile structures with a life span of ~10 s (Smith et al., 2001; Carlsson et al., 2002). Second, most patches display random motion and a few display directed motion. Third, patches have an average speed of 0.49 ± 0.30 μm/s. Together, most patches would have disassembled before they can cross the bud neck. Thus, it has been concluded that the organization of actin patches is due to the assembly of the patches at the sites of polarized growth (Smith et al., 2001). The lifespan of actin patches in different mutants cannot explain the observed phenotype either, because the lifespan of the patches in *sec6–4 tpm1–2 tpm2Δ* cells increases only two-fold over that in *tpm1–2 tpm2Δ* cells at 36°C.

The patch polarization in *sec6–4 tpm1–2 tpm2Δ* cells and patch organization in general can be explained by assuming that secretory vesicles carry factors that are required for actin-patch clustering and/or assembly; and that local concentration of these factors depends on the balance of exocytosis and endocytosis (Fig. 7 B). During bud growth of wild-type cells, exocytosis prevails over endocytosis; these factors accumulate dynamically at the sites of polarized growth, leading to polarized actin-patch organization. In the tropomyosin mutants, these putative factors are deposited over the entire cell surface through ongoing depolarized exocytosis, and the high concentration of these factors at the "old buds" is eliminated through active endocytosis, which is not blocked in these mutants (Pruyne et al., 1998); thus, leading to the reorganization of actin patches. In the *sec6–4 tpm1–2 tpm2Δ* and *sec6–4* mutants, exocytosis and endocytosis are blocked together, the high concentration of the putative factors in the old buds remains; thus, actin patches are still polarized, and are still going through their dynamic assembly and disassembly cycle. These putative factors could include polarity proteins such as Cdc42p and Rho1p, and actin-binding proteins such as Aip3p/Bud6p, because their accumulation at the active growth sites depends on intact secretory pathway (McCaffrey et al., 1991; Jin and Amberg, 2000; Wedlich-Soldner et al., 2003).

Our finding on the cause-effect relationship between vesicle fusion and the organization of actin patches has profound biological implications. Exocytosis and endocytosis are intimately coupled in many biological systems including *S. cerevisiae* (Riezman, 1985), *Drosophila* (Roos and Kelly, 1999), and

Table III. **Yeast strains used in this study**

Name	Genotype	Source
YEF473	**a**/α *his3/his3 leu2/leu2 lys2/lys2 trp1/trp1 ura3/ura3*	(Bi and Pringle, 1996)
YEF473A	**a** *his3 leu2 lys2 trp1 ura3*	Segregant from YEF473
YEF115	α *his4 leu2 trp1 ura3 gal2 cdc42-1*	J. Pringle
YEF1264	As YEF473 except *MSB3/msb3Δ::HIS3 MSB4/msb4Δ::TRP1*	(Bi et al., 2000)
YEF1289	**a** *his3 leu2 lys2 trp1 ura3 msb3Δ::HIS3 msb4Δ::TRP1*	(Bi et al., 2000)
YEF1291	α *his3 leu2 lys2 trp1 ura3 msb3Δ::HIS3 msb4Δ::TRP1*	(Bi et al., 2000)
YEF1563	As YEF473 except *MSB3/msb3Δ::HIS3 MSB4/msb4Δ::HIS3 GIC1/gic1-Δ1::LEU2 GIC2/gic2-Δ2::TRP1*	YEF1269 × CCY1042-12B
YEF1619	As YEF473 except *msb3Δ::HIS3/msb3Δ::TRP1*	YEF1239 × YEF1304
YEF1631	As YEF473 except *msb3Δ::HIS3/msb3Δ::HIS3 msb4Δ::TRP1/msb4Δ::TRP1*	(Bi et al., 2000)
YEF2258	**a** *his3 leu2 lys2 trp1 ura3 cdc42-201*	(Zhang et al., 2001)
ABY971	As ABY973 except *tpm1-2::LEU2/tpm1-2::LEU2*	(Pruyne et al., 1998)
ABY973	**a**/α *tpm2Δ::HIS3/tpm2Δ::HIS3 his3Δ-200/his3Δ-200 leu2-3,112/leu2-3,112 lys2-801/lys2-801 trp1-1/trp1-1 ura3-52/ura3-52*	(Pruyne et al., 1998)
ABY999	As ABY973 except *tpm1-2::LEU2/tpm1-2::LEU2 sec6-4/sec6-4 SEC8:HA3::TRP1/SEC8:HA3::TRP1*	(Pruyne et al., 1998)
BY37	**a** *ura3-52 sec6-4*	P. Brennwald
BY45	**a** *ura3-52 sec15-1*	P. Brennwald
JGY10	**a** *his3 leu2 lys2 trp1 ura3 msb3Δ::HIS3 msb4Δ::HIS3 gic1-Δ1::kanMX6 gic2-Δ2::TRP1* (pCC904-GIC1)	This study
JGY18	**a** *his3 leu2 lys2 trp1 ura3 msb3Δ::HIS3 msb4Δ::TRP1 cdc42-201* (pRS316-CDC42)	Segregant from JGY13
JGY28B	α *his3 leu2 trp1 ura3 sec2-41*	This study
JGY30A	**a** *his3 leu2 trp1 ura3 sec6-4*	This study
JGY31B	α *his3 leu2 trp1 ura3 sec9-4*	This study
JGY32B	α *his3 leu2 trp1 ura3 sec3-2*	This study
JGY37B	α *his3 leu2 trp1 ura3 sec3-2 msb3Δ::HIS3 msb4Δ::TRP1*	This study
JGY39A	**a** *his3 leu2 lys2 trp1 ura3 sec6-4 msb3Δ::HIS3 msb4Δ::TRP1*	This study
JGY40A	**a** *his3 leu2 lys2 trp1 ura3 sec9-4 msb3Δ::HIS3 msb4Δ::TRP1*	This study
JGY48A	**a** *his3 leu2 lys2 trp1 ura3 sec4Δ::kanMX6* (pRS316-SEC4)	This study
JGY51	**a** *msb3Δ::HIS3 msb4Δ::3HA-MSB4 his3 leu2 lys2 trp1 ura3*	This study
JGY71	As YEF473 except *msb3Δ::HIS3/msb3Δ::HIS3 msb4Δ::3HA-MSB4/msb4Δ::3HA-MSB4*	This study
JGY73	**a** *his3 leu2 lys2 trp1 ura3 sec4-Q79L*	This study
JGY82B	α *his3 leu2 trp1 ura3 sec15-1*	This study
JGY86A	**a** *his3 leu2 trp1 ura3 sec15-1 sec4-Q79L* (pRS316-SEC4)	This study
JGY127A	**a** *msb3Δ::HIS3 msb4Δ::3HA-MSB4-R200K his3 leu2 lys2 trp1 ura3*	This study
JGY130	As YEF473 except *msb3Δ::HIS3/msb3Δ::HIS3 msb4Δ::3HA-MSB4-R200K/msb4Δ::3HA-MSB4-R200K*	This study
JGY184A	**a** *msb3Δ::3HA-MSB3 msb4Δ::TRP1 his3 leu2 lys2 trp1 ura3*	This study
JGY184	As YEF473 except *msb3Δ::3HA-MSB3/msb3Δ::3HA-MSB3 msb4Δ::TRP1/msb4Δ::TRP1*	This study
JGY190A	**a** *msb3Δ::3HA-MSB3-R282K msb4Δ::TRP1 his3 leu2 lys2 trp1 ura3*	This study
JGY190	As YEF473 except *msb3Δ::3HA-MSB3-R282K/msb3Δ::3HA-MSB3-R282K msb4Δ::TRP1/msb4Δ::TRP1*	This study
JGY381	**a**/α *his3/his3 leu2/leu2 ura3/ura3 TRP1/trp1 sec6-4/sec6-4*	This study

mammals (Sudhof, 2000), but the mechanisms are unclear. In *S. cerevisiae*, many components of the actin patches are required for the internalization step of endocytosis (Munn, 2000); thus, our finding could provide a concrete means to spatially link exocytosis to endocytosis (Fig. 7, A and B): fusion of the exocytic vesicles with the plasma membranes leads to the clustering of actin patches at the fusion site, which mediate endocytosis to recycle the exocytic machinery. This finding also explains why the actin patches and the ends of the actin cables, which mediate exocytosis, are always in close proximity with each other (Karpova et al., 1998).

Materials and methods

Strains and media

Yeast strains used in this study are listed in Table III. Standard culture media and genetic techniques were used (Guthrie and Fink, 1991). 1 mg/ml 5-fluroorotic acid (5FOA) (Angus Buffers and Biochemicals) was added to media to select for the loss of *URA3*-containing plasmids.

Construction of plasmids and DNA mutagenesis

Plasmids used in this study include YEplac181 (2 μ, *LEU2*), pRS316 (*CEN, URA3*), pFA6a-kanMX6 (Longtine et al., 1998), pYES2-MSB3 (Albert and Gallwitz, 1999), pET22-MSB4 (Albert and Gallwitz, 2000), YEp181–3HA-MSB3 and YEp181–3HA-MSB4 (Bi et al., 2000), pCC904-GIC1 (2 μ, *URA3*) (Bi et al., 2000), pRS316-CDC42 (Bi and Pringle, 1996), and pRS423-SEC4 (2 μ, *HIS3*). Plasmids YEp181-SEC4 and pRS316-SEC4 were constructed by inserting a 1.5-kb BamHI-EcoRI fragment carrying *SEC4* from pRS423-SEC4 into YEplac181 and pRS316 at the corresponding sites, respectively. *GYP1* (from −561 to 2,310) was cloned into YEplac181 vector by plasmid gap-repair. Change of arginine to phenylalanine or lysine codon in *MSB3* and *MSB4* was achieved by using Quikchange site-directed mutagenesis kit (Stratagene). The Q79L mutation in *SEC4* was introduced into YEp181-SEC4 by a PCR-based method. All intended mutations, including *msb3-R282F*, *msb3-R282K*, *msb4-R200F*, *msb4-R200K*, and *sec4-Q79L*, were confirmed by DNA sequencing.

Construction of yeast strains

To construct strain JGY10 for our first functional assay, the *LEU2* gene marking the *gic1-Δ1* deletion in YEF1563 (Bi et al., 2000) was replaced precisely with *kanMX6* by a PCR-based method (Longtine et al., 1998). The resulting heterozygote (*GIC1/gic1-Δ1::kanMX6*) carrying plasmid

pCC904-GIC1 was sporulated to generate JGY10. To construct JGY18 for our second assay, YEF1291 was crossed to YEF2258 carrying pRS316-CDC42. The resulting heterozygote was sporulated to generate JGY18.

To construct JGY28B (*sec2–41*), JGY30A (*sec6–4*), JGY31B (*sec9–4*), JGY32B (*sec3–2*), and JGY82B (*sec15–1*) strains, we crossed wild-type strains from our laboratory (YEF473A or YEF473B) with strains bearing these mutations in another genetic background and isolated segregants of desirable genotypes. Appropriate segregants from one of theses crosses were mated to generate JGY381 (*sec6–4/sec6–4*). Triple mutants JGY37B (*sec3–2 msb3Δ msb4Δ*), JGY39A (*sec6–4 msb3Δ msb4Δ*), and JGY40A (*sec9–4 msb3Δ msb4Δ*) were isolated from crosses between individual *sec* mutants and haploid *msb3Δ msb4Δ* cells.

To construct a strain carrying *sec4-Q79L*, one copy of *SEC4* in YEF473 was replaced with *KanMX6* by the PCR-mediated method (Longtine et al., 1998). The resulting heterozygote carrying pRS316-SEC4 was sporulated to generate JGY48A. The 1.5-kb BamHI-EcoRI fragment containing *sec4-Q79L* was transformed into JGY48A, and colonies that were 5FOA-resistant and G418-sensitive were selected, generating JGY73. JGY86A was a segregant from the cross between JGY82B (*sec15–1*) and JGY73 (*sec4-Q79L*) carrying pRS316-SEC4.

To construct strains JGY184 and JGY190, we integrated Tth111I-digested plasmids YIplac-3HA-MSB3 (Bi et al., 2000) and YIplac-3HA-MSB3-R282K at the Tth111I site (−401 position) upstream of the *msb3Δ* locus in YEF1264. The correctness of the transformants was confirmed by the linkage of *HIS3* and *URA3* markers in every single segregant and by the expression of HA-tagged proteins. Strains of opposite mating types with desired genotypes were crossed to generate JGY184 and JGY190. Similarly, strains JGY71 and JGY130 were constructed by integrating EcoNI-digested plasmids YIplac-3HA-MSB4 (Bi et al., 2000) and YIplac-3HA-MSB4-R200K at the EcoNI site (−639 position) upstream of the *msb4Δ* locus in YEF1264.

Production of Msb3p and Msb4p proteins and measurement of their GAP activity

Production of His_6-tagged Msb3p and its arginine mutants from yeast, and His_6-tagged Msb4p and its arginine mutants from *E. coli*, and measurement of the GAP activity were all performed as described previously (Albert and Gallwitz, 1999; Albert and Gallwitz, 2000).

Immunoblotting and immunofluorescence microscopy

For immunoblotting, the mouse monoclonal anti-HA antibody HA.11 (Berkeley Antibody Company), or the rabbit anti-Isp42p polyclonal antibodies were used. Proteins were detected with the ECL Western blotting detection reagents.

For localization of HA-tagged Msb3p or Msb4p, yeast cells grown exponentially in SC-Leu media at 24°C were fixed by formaldehyde and processed for immunofluorescence microscopy as described by Pringle et al. (1991). Mouse anti-HA antibody HA.11 and the secondary Cy3-conjugated donkey anti–mouse IgG antibody were used. For visualizing the actin cytoskeleton, yeast cells were fixed with 4% formaldehyde for 1 h at 24°C and stained with rhodamine-phalloidin (Molecular Probes). DNA was stained with 1 μg/ml bisBenzimide (Sigma-Aldrich). Differential interference contrast (DIC) and fluorescence microscopy were performed using Nikon Microscope ECLIPSE E800 (Nikon Corporation) with a 60× plan apo objective. The images were acquired using Image-Pro Plus software (Media Cybernetics).

Electron microscopy

Yeast cells were grown in YPD media to early log phase at 24°C. For *cdc42*-Ts mutants, cells grown exponentially at 24°C were shifted to restrictive temperatures for 1 h, and were prefixed with 1.6% of glutaraldehyde in culture for 10 min. 10–20-A_{600} units of cells were fixed in 1 ml fixative (2% glutaraldehyde in PBS buffer, pH 7.4) at 24°C for 30 min, which was followed by additional 30 min with fresh fixative. Cells were then spheroplasted and fixed with 1% glutaraldehyde (in PBS buffer, pH 7.4) at 4°C overnight. Spheroplasts were washed in 0.1 M cacodylate buffer and postfixed twice with ice-cold solution containing 0.5% OsO_4 and 0.8% potassium ferricyanide on ice for 10 min each time. Spheroplasts were then washed with dH_2O and incubated in 2% uranyl acetate at 24°C for 30 min in dark, which was followed by standard dehydration. Cell pellets were embedded in Spurr's resin. Thin sections were cut and processed for electron microscopy. Cells were viewed with a JEOL 1010 electron microscope and photographed at 80 kV. The size of vesicles was measured at 100,000× magnification.

Invertase secretion assay

Yeast cells were grown to exponential phase in YPD media containing 5% dextrose at 24°C. Approximately 1.5-A_{600} units of cells were collected, washed twice with YPD media containing 0.1% dextrose, and resuspended in 1.5 ml of the same media. Secretion of invertase was induced for various time at 24°C. Cells from each time point were washed with and resuspended in 1 ml of ice-cold 10 mM NaN_3 solution. A_{600} of this cell suspension was measured. 20 μl of cell suspension was directly applied to assay external (periplasmic) pool of invertase. For assaying the internal (intracellular) pool of invertase, 0.5 ml cell suspension was mixed with 0.5 ml 2× spheroplast cocktail mix (2.8 M sorbitol, 0.1 M Tris-HCl, 10 mM NaN_3, pH 7.5, 0.4% β-mercaptoethanol) and 50 μl 10 mg/ml lyticase to remove the cell wall. Spheroplasts were lysed in 0.5 ml 0.5% Triton X-100. The lysate was centrifuged at 14,000 rpm for 10 min at 4°C. 20 μl of supernatant was used to assay internal pool of invertase. The external and internal pools of invertase activity were assayed by following the protocol described by Adamo et al. (1999).

Bgl2p secretion assay

Yeast cells were grown to midlog phase at 24°C. Half of the culture was kept at 24°C and the other half was shifted to 37°C for 1 h. At the end of shift, NaN_3 and NaF were added to ~20 mM each to all cultures. 25-A_{600} units of cells from each culture were washed in 20 mM NaN_3/20 mM NaF twice and resuspended in 830 μl of spheroplasting solution (100 mM Tris-HCl, pH 7.5, 1.6 M sorbitol, 12 mM NaN_3, 0.1% β-mercaptoethanol, 200 μg/ml zymolyase 100-T). Spheroplasts were gently pelleted at 2,000 rpm for 5 min. The top 830 μl of the supernatant (external Bgl2p pool) was transferred to a new tube and 170 μl of 6× sample buffer (0.35 M Tris-HCl, pH 6.8, 30% glycerol, 10% SDS, 93 mg/ml DTT, 0.1 mg/ml bromphenol blue) was added to it, and the samples were boiled immediately for 10 min. The pellet (internal Bgl2p pool) was resuspended in 1 ml of 2× sample buffer and boiled for 10 min 50 μl of samples were separated by a 12.5% SDS-polyacrylamide gel, probed with a rabbit α-Bgl2p antibody, and detected by ECL.

Enrichment of unbudded cells

Cdc42-Ts mutant cells harboring YEplac181-based plasmids were grown on SC-Leu plates at 24°C for 4 d. Cells were then scraped off plates and resuspended in 25 ml of 1 M sorbitol + 50% SC-Leu. Unbudded cells were enriched by repeated centrifugation at 800 rpm for 1 min until more than 90% of cells was unbudded. 5–10-A_{600} units of the enriched cells were transferred into 40 ml SC-Leu media and incubated at restrictive temperatures until ~50% cells from the positive samples became budded. Cells were then fixed with 4% formaldehyde at the restrictive temperatures for 15 min. For 24°C controls, the remaining enriched cells were fixed in 4% formaldehyde at 24°C for 1 h. Fixed cells were stained for F-actin and DNA.

Determination of the organization and life span of actin patches

To determine actin-patch organization, an *URA3*-marked integrative plasmid pASF125 carrying an NH_2-terminal tagged *GFP-TUB1* was linearlized by StuI and integrated at the *ura3* locus in yeast strains ABY971, ABY973, ABY999, and JGY381, respectively. The resulting strains were inoculated in 50 ml YPD media and incubated at 24°C until A_{600} reached 0.2–0.4. Approximately 4-A_{600} units of cells were diluted into 20 ml YPD and incubated in a water-bath shaker at 36°C. After incubation at 36°C for 30 min or 60 min, formaldehyde was added directly into cultures to 4% final concentration. Fixed cells were stained for F-actin. Only small-budded cells with a short spindle were scored for actin-patch organization.

To determine the lifespan of actin patches, plasmid pRB2139 carrying *ABP1-GFP* was transformed into strains ABY971, ABY973, ABY999, and JGY381, respectively. 5 μl of exponentially growing cells in SC-Ura medium at 20°C were spotted onto a flat agarose patch that contains the same medium with 2% agarose on a microscope slide, covered with a cover glass, and sealed with nail polish. Time-lapse series were obtained with a computer-controlled Nikon E800 microscope and with a digital camera (model 4742-95; Hamamatsu Photogenics), using the Image-Pro Plus software. 31 images of each cell expressing Abp1p-GFP were acquired in a single focal plane at 20°C and at 36°C using 0.5-s exposure and 2-s interval. For 36°C studies, sealed slides were preincubated in a moistened chamber at 36°C for 60 min, and quickly put under an objective lens heated to 36°C during the course of the time-lapse study. Images were analyzed using NIH ImageJ 1.29 software (http://rsb.info.nih.gov/). The lifespan of an Abp1p-GFP patch is defined as the period between the first frame that it appears and the first frame that it becomes completely invisible. Only budded cells, including the mother and daughter compartments, were analyzed.

We thank Drs. P. Brennwald, D. Pruyne, A. Bretscher, D. Amberg, and J. Pringle for providing antibody, plasmids, and yeast strains; U. Welscher-

Altschäffel and N. Shah for expert technical assistance; and Drs. D. Lew, S. Zigmond, and M. Chou for critically reading the manuscript.

This work was supported by National Institutes of Health grants GM59216 to E. Bi. and GM61221 to C. Burd, the Max Planck Society, and grants to D. Gallwitz from the Deutsche Forschungsgemeinschaft and Fonds der Chemischen Industrie and Human Frontier Science Program.

Submitted: 6 February 2003
Accepted: 10 July 2003

References

Adamo, J.E., G. Rossi, and P. Brennwald. 1999. The Rho GTPase Rho3 has a direct role in exocytosis that is distinct from its role in actin polarity. *Mol. Biol. Cell.* 10:4121–4133.

Adamo, J.E., J.J. Moskow, A.S. Gladfelter, D. Viterbo, D.J. Lew, and P.J. Brennwald. 2001. Yeast Cdc42 functions at a late step in exocytosis, specifically during polarized growth of the emerging bud. *J. Cell Biol.* 155:581–592.

Ahmadian, M.R., P. Stege, K. Scheffzek, and A. Wittinghofer. 1997. Confirmation of the arginine-finger hypothesis for the GAP-stimulated GTP-hydrolysis reaction of Ras. *Nat. Struct. Biol.* 4:686–689.

Albert, S., and D. Gallwitz. 1999. Two new members of a family of Ypt/Rab GTPase activating proteins. Promiscuity of substrate recognition. *J. Biol. Chem.* 274:33186–33189.

Albert, S., and D. Gallwitz. 2000. Msb4p, a protein involved in Cdc42p-dependent organization of the actin cytoskeleton, is a Ypt/Rab-specific GAP. *Biol. Chem.* 381:453–456.

Albert, S., E. Will, and D. Gallwitz. 1999. Identification of the catalytic domains and their functionally critical arginine residues of two yeast GTPase-activating proteins specific for Ypt/Rab transport GTPases. *EMBO J.* 18:5216–5225.

Bender, A., and J.R. Pringle. 1989. Multicopy suppression of the *cdc24* budding defect in yeast by *CDC42* and three newly identified genes including the *ras*-related gene *RSR1*. *Proc. Natl. Acad. Sci. USA.* 86:9976–9980.

Bi, E., J.B. Chiavetta, H. Chen, G.-C. Chen, C.S.M. Chan, and J.R. Pringle. 2000. Identification of novel, evolutionarily conserved Cdc42p-interacting proteins and of redundant pathways linking Cdc24p and Cdc42p to actin polarization in yeast. *Mol. Biol. Cell.* 11:773–793.

Bi, E., and J.R. Pringle. 1996. *ZDS1* and *ZDS2*, genes whose products may regulate Cdc42p in *Saccharomyces cerevisiae*. *Mol. Cell. Biol.* 16:5264–5275.

Carlsson, A.E., A.D. Shah, D. Elking, T.S. Karpova, and J.A. Cooper. 2002. Quantitative analysis of actin patch movement in yeast. *Biophys. J.* 82:2333–2343.

De Antoni, A., J. Schmitzova, H.-H. Trepte, D. Gallwitz, and S. Albert. 2002. Significance of GTP hydrolysis in Ypt1p-regulated ER to Golgi transport revealed by analysis of two novel Ypt1-GAPs. *J. Biol. Chem.* 277:41023–41031.

Drubin, D.G., and W.J. Nelson. 1996. Origins of cell polarity. *Cell.* 84:335–344.

Du, L.L., R.N. Collins, and P.J. Novick. 1998. Identification of a Sec4p GTPase-activating protein (GAP) as a novel member of a Rab GAP family. *J. Biol. Chem.* 273:3253–3256.

Du, L.L., and P. Novick. 2001. Yeast Rab GTPase-activating protein Gyp1p localizes to the Golgi apparatus and is a negative regulator of Ypt1p. *Mol. Biol. Cell.* 12:1215–1226.

Guo, W., D. Roth, C. Walch-Solimena, and P. Novick. 1999. The exocyst is an effector for Sec4p, targeting secretory vesicles to sites of exocytosis. *EMBO J.* 18:1071–1080.

Guthrie, C., and G.R. Fink, editors. 1991. Guide to yeast genetics and molecular biology. *In* Methods in Enzymology, Vol. 194. Academic Press, San Diego. 933 pp.

Harsay, E., and A. Bretscher. 1995. Parallel secretory pathways to the cell surface in yeast. *J. Cell Biol.* 131:297–310.

Jin, H., and D.C. Amberg. 2000. The secretory pathway mediates localization of the cell polarity regulator Aip3p/Bud6p. *Mol. Biol. Cell.* 11:647–661.

Johnson, D.I. 1999. Cdc42: an essential Rho-type GTPase controlling eukaryotic cell polarity. *Microbiol. Mol. Biol. Rev.* 63:54–105.

Karpova, T.S., J.G. McNally, S.L. Moltz, and J.A. Cooper. 1998. Assembly and function of the actin cytoskeleton of yeast: relationships between cables and patches. *J. Cell Biol.* 142:1501–1517.

Longtine, M.S., A. McKenzie, III, D.J. DeMarini, N.G. Shah, A. Wach, A. Brachat, P. Philippsen, and J.R. Pringle. 1998. Additional modules for versatile and economical PCR-based gene deletion and modification in *Saccharomyces cerevisiae*. *Yeast.* 14:953–961.

McCaffrey, M., J.S. Johnson, B. Goud, A.M. Myers, J. Rossier, M.R. Popoff, P. Madaule, and P. Boquet. 1991. The small GTP-binding protein Rho1p is localized on the Golgi apparatus and post-Golgi vesicles in *Saccharomyces cerevisiae*. *J. Cell Biol.* 115:309–319.

Mrsa, V., F. Klebl, and W. Tanner. 1993. Purification and characterization of the *Saccharomyces cerevisiae BGL2* gene product, a cell wall endo-beta-1,3-glucanase. *J. Bacteriol.* 175:2102–2106.

Munn, A.L. 2000. The yeast endocytic membrane transport system. *Microsc. Res. Tech.* 51:547–562.

Novick, P., and R. Schekman. 1979. Secretion and cell-surface growth are blocked in a temperature-sensitive mutant of *Saccharomyces cerevisiae*. *Proc. Natl. Acad. Sci. USA.* 76:1858–1862.

Pringle, J.R., A.E.M. Adams, D.G. Drubin, and B.K. Haarer. 1991. Immunofluorescence methods for yeast. *Methods Enzymol.* 194:565–602.

Pruyne, D., and A. Bretscher. 2000a. Polarization of cell growth in yeast. *J. Cell Sci.* 113:571–585.

Pruyne, D., and A. Bretscher. 2000b. Polarization of cell growth in yeast. I. Establishment and maintenance of polarity states. *J. Cell Sci.* 113:365–375.

Pruyne, D.W., D.H. Schott, and A. Bretscher. 1998. Tropomyosin-containing actin cables direct the Myo2p-dependent polarized delivery of secretory vesicles in budding yeast. *J. Cell Biol.* 143:1931–1945.

Riezman, H. 1985. Endocytosis in yeast: several of the yeast secretory mutants are defective in endocytosis. *Cell.* 40:1001–1009.

Roos, J., and R.B. Kelly. 1999. The endocytic machinery in nerve terminals surrounds sites of exocytosis. *Curr. Biol.*:1411-1414.

Smith, M.G., S.R. Swamy, and L.A. Pon. 2001. The life cycle of actin patches in mating yeast. *J. Cell Sci.* 114:1505–1513.

Strom, M., P. Vollmer, T.J. Tan, and D. Gallwitz. 1993. A yeast GTPase-activating protein that interacts specifically with a member of the Ypt/Rab family. *Nature.* 361:736–739.

Sudhof, T.C. 2000. The synaptic vesicle cycle revisited. *Neuron.* 28:317–320.

Vollmer, P., and D. Gallwitz. 1995. High expression cloning, purification, and assay of Ypt-GTPase-activating proteins. *Methods Enzymol.* 257:118–128.

Vollmer, P., E. Will, D. Scheglmann, M. Strom, and D. Gallwitz. 1999. Primary structure and biochemical characterization of yeast GTPase-activating proteins with substrate preference for the transport GTPase Ypt7p. *Eur. J. Biochem.* 260:284–290.

Walch-Solimena, C., R.N. Collins, and P.J. Novick. 1997. Sec2p mediates nucleotide exchange on Sec4p and is involved in polarized delivery of post-Golgi vesicles. *J. Cell Biol.* 137:1495–1509.

Walworth, N.C., P. Brennwald, A.K. Kabcenell, M. Garrett, and P. Novick. 1992. Hydrolysis of GTP by Sec4 protein plays an important role in vesicular transport and is stimulated by a GTPase-activating protein in *Saccharomyces cerevisiae*. *Mol. Cell. Biol.* 12:2017–2028.

Wedlich-Soldner, R., S. Altschuler, L. Wu, and R. Li. 2003. Spontaneous cell polarization through actomyosin-based delivery of the Cdc42 GTPase. *Science.* 299:1231–1235.

Zhang, X., E. Bi, P. Novick, L. Du, K.G. Kozminski, J.H. Lipschutz, and W. Guo. 2001. Cdc42 interacts with the exocyst and regulates polarized secretion. *J. Biol. Chem.* 276:46745–46750.